2996 *Inorg. Chem.* **2010**, *49*, 2996–3001
DOI: 10.1021/ic902511m

Inorganic Chemistry
Article

Major Difference between the Isoelectronic Fluoroborylene and Carbonyl Ligands: Triply Bridging Fluoroborylene Ligands in $Fe_3(BF)_3(CO)_9$ Isoelectronic with $Fe_3(CO)_{12}$

Liancai Xu,[†] Qian-shu Li,*[,†,‡] Yaoming Xie,[§] R. Bruce King,*[,†,§] and Henry F. Schaefer, III[§]

[†]*Center for Computational Quantum Chemistry, South China Normal University, Guangzhou 510631, P.R. China,* [‡]*Institute of Chemical Physics, Beijing Institute of Technology, Beijing 100081, P.R. China, and* [§]*Department of Chemistry and Center for Computational Chemistry, University of Georgia, Athens, Georgia 30602*

Received December 17, 2009

The structure of $Fe_3(BF)_3(CO)_9$ is predicted to be very different than that of any of the isoelectronic homoleptic $M_3(CO)_{12}$ derivatives (M = Fe, Ru, Os). Thus the lowest energy $Fe_3(BF)_3(CO)_9$ structure by ~19 kcal/mol has μ_3-BF groups bridging the top and bottom of the Fe_3 triangle with a third edge-bridging BF group in addition to nine terminal carbonyl groups. No analogous $M_3(CO)_{12}$ structures are found with μ_3-CO groups bridging the M_3 triangle. Higher energy $Fe_3(BF)_3(CO)_9$ structures with two edge-bridging μ-BF groups and one terminal BF group are also found, analogous to the experimentally known $Fe_3(CO)_{12}$ structure. However, these structures are transition states leading to local minima with one unsymmetrical face-bridging μ_3-BF group, one edge-bridging μ-BF group, and one terminal BF group. No $Fe_3(BF)_3(CO)_9$ structures are found with exclusively terminal BF and CO groups analogous to the known structures of $M_3(CO)_{12}$ (M = Ru, Os). These studies suggest that the BF group has a significantly greater tendency than the CO group to bridge two or three metal atoms, probably owing to the reluctance of the fluorine of the BF ligands to be a part of a formal double or triple bond.

1. Introduction

The fluoroborylene ligand, BF, is of interest since it is isoelectronic with the carbonyl ligand, CO, found in extensive series of metal carbonyl derivatives.[1] In this connection, metal carbonyl chemistry is highly developed, owing at least partially to the ready availability of carbon monoxide as a stable gas that can be used to introduce carbonyl groups into a variety of compounds.

The corresponding chemistry of metal fluoroborylene complexes is very limited. Although the free BF ligand (boron monofluoride) is obtained in high yield in the gas phase by passing BF_3 over crystalline boron at 2000°/1 mm,[2] it is unstable even in the gas phase and condenses to a green uncharacterized polymer, even at −196 °C. This instability of BF makes it unsuitable for a reagent to synthesize metal fluoroborylene complexes. For this reason, transition metal BF complexes need to be synthesized by indirect methods. In this connection the first mention of a metal BF complex is the synthesis of $Fe(BF)(CO)_4$ from $Fe(CO)_5$ and B_2F_4 reported in a 1968 conference proceedings.[3] In addition, another metal BF complex $Fe(PF_3)_4(BF)$ was characterized spectroscopically by Timms in 1972.[4] However, these studies have apparently not been repeated during the subsequent ~40 years and thus must be regarded as doubtful until they are confirmed. Much more relevant, the fluoroborylene ruthenium complex $Cp_2Ru_2(CO)_4(\mu$-BF) has been reported very recently (2009) by Vidović and Aldridge and characterized structurally by X-ray crystallography.[5] The structure of $Cp_2Ru_2(CO)_4(\mu$-BF) is of interest since the two ruthenium atoms are bridged by the BF ligand without an accompanying ruthenium−ruthenium bond. An analogous structural feature is not found in metal carbonyl chemistry, where bridging carbonyl groups are always accompanied by formal metal−metal bonding between the same metals bridged by the carbonyl group. This is one important difference between metal carbonyl and metal fluoroborylene chemistry. Recently, related transition-metal complexes containing the terminal GaI ligand have been synthesized.[6−8]

*To whom correspondence should be addressed. E-mail: rbking@chem.uga.edu.

(1) Cotton, F. A.; Wilkinson, G. *Advanced Inorganic Chemistry*; Wiley: New York, 1988; Chapter 22.
(2) Timms, P. L. *J. Am. Chem. Soc.* **1967**, *89*, 1629.
(3) Kämpfer, K.; Nöth, H.; Petz, W.; Schmid, G. *Proceedings of the First International Symposium on New Aspects of the Chemistry of Metal Carbonyl Derivatives*; Inorganica Chimica Acta: Padova, Italy, 1968.
(4) Timms, P. L. *Acc. Chem. Res.* **1973**, *6*, 118.
(5) Vidović, D.; Aldridge, S. *Angew. Chem., Int. Ed.* **2009**, *48*, 3669.
(6) Coombs, N. D.; Clegg, W.; Thompson, A. L.; Willock, D. J.; Aldridge, S. *J. Am. Chem. Soc.* **2008**, *130*, 5449.
(7) Coombs, N. D.; Vidović, D.; Day, J. K.; Thompson, A. L.; Le Pevelen, D. D.; Stasch, A.; Clegg, W.; Russo, L.; Male, L.; Hursthouse, M. B.; Willock, D. J.; Aldridge, S. *J. Am. Chem. Soc.* **2008**, *130*, 16111.
(8) Himmel, H.-J.; Linti, G. *Angew. Chem., Int. Ed.* **2008**, *47*, 6326.

Published on Web 02/09/2010

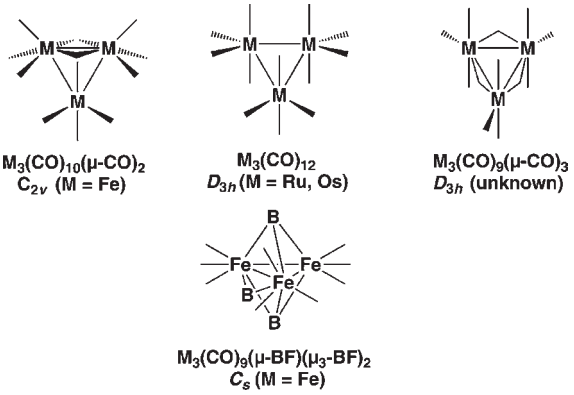

Figure 1. Comparison of the $M_3(CO)_{12}$ structures with the lowest energy structure found for $Fe_3(BF)_3(CO)_9$ (carbonyl groups and fluorine atoms omitted for clarity).

This paper reports another significant difference between the chemistry of CO and BF groups arising in their coordination to metal triangles. The prototypical examples of triangular metal carbonyl clusters are the $M_3(CO)_{12}$ derivatives (M = Fe, Ru, Os). The iron derivative $Fe_3(CO)_{12}$ was first reported more than a century ago by Dewar and Jones,[9] although its trinuclear nature was established only later by a cryoscopic molecular weight determination using $Fe(CO)_5$ as a solvent.[10,11] The definitive determination of the structure of $Fe_3(CO)_{12}$ using X-ray crystallography posed some disorder difficulties.[12] These difficulties were eventually resolved leading to a triangular $Fe_3(CO)_{12}$ structure (Figure 1) in which one of the three Fe−Fe edges of the triangle is bridged by a pair of carbonyl groups.[13,14] The analogous ruthenium and osmium derivatives were shown originally by their infrared ν(CO) spectra and later by X-ray crystallography to have a different structure in which all 12 carbonyl groups are terminal carbonyl groups (Figure 1).[15−17]

Recently we have been using density functional theory (DFT) methods to explore possible structures of other trinuclear metal carbonyl derivatives related to these $M_3(CO)_{12}$ derivatives. For $Fe_3(CS)_3(CO)_9$ the lowest energy structure is predicted to be a doubly bridged structure in which one of the edges of the underlying Fe_3 triangle is bridged by two CS groups.[18] However, in this case four other doubly bridged structures were found within ~5 kcal/mol of the global minimum. Each of these four structures has one of the edges of the Fe_3 triangle bridged by two CE (E = S, O) groups, with the CS-bridged structures being of slightly lower energy than the CO-bridged structures. The greater tendency of a CS group to bridge a pair of metal atoms than a CO group is also predicted by DFT studies of binuclear $M_2(CS)_2(CO)_n$ derivatives of other first-row transition metals such as manganese,[19] iron,[20] and cobalt.[21] For $Fe_3(CS)_3(CO)_9$ the lowest energy unbridged structure analogous to the lowest energy $M_3(CO)_{12}$ structures (M = Ru, Os) is predicted to lie ~20 kcal/mol above the doubly CS-bridged global minimum.

This paper reports an analogous DFT study on $Fe_3(BF)_3(CO)_9$. The results were found to be surprising since the lowest energy $Fe_3(BF)_3(CO)_9$ structure is like neither the doubly bridged $Fe_3(CO)_{12}$ structure nor the unbridged $M_3(CO)_{12}$ (M = Ru, Os) structures. Instead, an unprecedented $Fe_3(CO)_9(\mu\text{-BF})(\mu_3\text{-BF})_2$ structure is found with two μ_3-BF groups each bridging all three iron atoms of the Fe_3 triangle and the third μ-BF group bridging one of the edges of the Fe_3 triangle (Figure 1). Furthermore, this $Fe_3(BF)_3(CO)_9$ structure is predicted to be favored over the next lower energy structure by ~20 kcal/mol.

2. Theoretical Methods

Electron correlation effects were considered using density functional theory (DFT) methods, which have evolved as a practical and effective computational tool, especially for organometallic compounds.[22−36] Two DFT methods were used in this study. The popular B3LYP method combines the three-parameter Becke functional (B3) with the Lee−Yang−Parr (LYP) generalized gradient correlation functional.[37,38] The BP86 method combines Becke's 1988 exchange functional (B) with Perdew's 1986 gradient corrected correlation functional (P86).[39,40] The BP86 method has been found to be somewhat more reliable than B3LYP for the type of organometallic systems considered in this paper, especially for the prediction of vibrational frequencies.[41−43]

For comparison with our previous research, the same double-ζ plus polarization (DZP) basis sets were adopted in the present study. Thus one set of pure spherical harmonic d functions with orbital exponents α_d(B) = 0.7,

(9) Dewar, J.; Jones, H. O. *Proc. Roy. Soc.* **1907**, *79A*, 66.
(10) Hieber, W.; Becker, E. *Chem. Ber.* **1930**, *63*, 1405.
(11) Hieber, W. *Z. Anorg. Allgem. Chem.* **1932**, *203*, 165.
(12) Desiderato, R.; Dobson, G. R. *J. Chem. Educ.* **1982**, *59*, 752.
(13) Wei, C. H.; Dahl, L. F. *J. Am. Chem. Soc.* **1966**, *88*, 1821.
(14) Cotton, F. A.; Troup, J. M. *J. Am. Chem. Soc.* **1974**, *96*, 4155.
(15) Mason, R.; Rae, A. I. M. *J. Chem. Soc. A* **1968**, 778.
(16) Churchill, M. R.; DeBoer, B. G. *Inorg. Chem.* **1977**, *16*, 878.
(17) Corey, E. R.; Dahl, L. F. *J. Am. Chem. Soc.* **1961**, *83*, 2203.
(18) Zhang, Z.; Li, Q.-S.; Xie, Y.; King, R. B.; Schaefer, H. F. *Inorg. Chem.* **2009**, *48*, 6167.
(19) Zhang, Z.; Li, Q.-S.; Xie, Y.; King, R. B.; Schaefer, H. F. *New J. Chem.* **2010**, *34*, 92.
(20) Zhang, Z.; Li, Q.-S.; Xie, Y.; King, R. B.; Schaefer, H. F. *Inorg. Chem.* **2009**, *48*, 1974.
(21) Zhang, Z.; Li, Q.-S.; Xie, Y.; King, R. B.; Schaefer, H. F., III *Inorg. Chem.* **2009**, *48*, 5973.
(22) Ehlers, A. W.; Frenking, G. *J. Am. Chem. Soc.* **1994**, *116*, 1514.
(23) Delly, B.; Wrinn, M.; Lüthi, H. P. *J. Chem. Phys.* **1994**, *100*, 5785.
(24) Li, J.; Schreckenbach, G.; Ziegler, T. *J. Am. Chem. Soc.* **1995**, *117*, 486.
(25) Jonas, V.; Thiel, W. *J. Phys. Chem.* **1995**, *102*, 8474.
(26) Barckholtz, T. A.; Bursten, B. E. *J. Am. Chem. Soc.* **1998**, *120*, 1926.
(27) Niu, S.; Hall, M. B. *Chem. Rev.* **2000**, *100*, 353.
(28) Macchi, P.; Sironi, A. *Coord. Chem. Rev.* **2003**, *238*, 383.
(29) Buhl, M.; Kabrede, H. *J. Chem. Theory Comput.* **2006**, *2*, 1282.
(30) Tonner, R.; Heydenrych, G.; Frenking, G. *J. Am. Chem. Soc.* **2008**, *130*, 8952.
(31) Ziegler, T.; Autschbach, J. *Chem. Rev.* **2005**, *105*, 2695.
(32) Waller, M. P.; Bühl, M.; Geethanakshmi, K. R.; Wang, D.; Thiel, W. *Chem.—Eur. J.* **2007**, *13*, 4723.
(33) Hayes, P. G.; Beddie, C.; Hall, M. B.; Waterman, R.; Tilley, T. D. *J. Am. Chem. Soc.* **2006**, *128*, 428.
(34) Bühl, M.; Reimann, C.; Pantazis, D. A.; Bredow, T.; Neese, F. *J. Chem. Theory Comput.* **2008**, *4*, 1449.
(35) Besora, M.; Carreon-Macedo, J.-L.; Cowan, J.; George, M. W.; Harvey, J. N.; Portius, P.; Ronayne, K. L.; Sun, X.-Z.; Towrie, M. *J. Am. Chem. Soc.* **2009**, *131*, 3583.
(36) Ye, S.; Tuttle, T.; Bill, E.; Simkhorich, L.; Gross, Z.; Thiel, W.; Neese, F. *Chem.—Eur. J.* **2008**, *14*, 10839.
(37) Becke, A. D. *J. Chem. Phys.* **1993**, *98*, 5648.
(38) Lee, C.; Yang, W.; Parr, R. G. *Phys. Rev. B* **1988**, *37*, 785.
(39) Becke, A. D. *Phys. Rev. A* **1988**, *38*, 3098.
(40) Perdew, J. P. *Phys. Rev. B* **1986**, *33*, 8822.
(41) See especially: Furche, F.; Perdew, J. P. *J. Chem. Phys.* **2006**, *124*, 044103.
(42) Wang, H. Y.; Xie, Y.; King, R. B.; Schaefer, H. F. *J. Am. Chem. Soc.* **2005**, *127*, 11646.
(43) Wang, H. Y.; Xie, Y.; King, R. B.; Schaefer, H. F. *J. Am. Chem. Soc.* **2006**, *128*, 11376.

$\alpha_d(C) = 0.75$, $\alpha_d(O) = 0.85$, and $\alpha_d(F) = 1.0$ for boron, carbon, oxygen, and fluorine, respectively, was added to the standard Huzinaga−Dunning contracted DZ sets,[44−46] designated as (9s5p1d/4s2p1d). The loosely contracted DZP basis set for iron is the Wachters primitive set[47] augmented by two sets of p functions and one set of d functions, contracted following Hood, Pitzer and Schaefer,[48] designated as (14s11p6d/10s8p3d).

The geometries of all structures were fully optimized using the two DFT methods. Harmonic vibrational frequencies were determined by evaluating analytically the second derivatives of the energy with respect to the nuclear coordinates. All calculations were performed with the Gaussian 03 program package.[49] The fine grid (75, 302) was the default for the numerical evaluation of the integrals, while the finer grid (120, 974) was only used to evaluate the small imaginary vibrational frequencies.[50]

3. Results

3.1. Molecular Structures. Eight optimized singlet structures and one triplet structure for $Fe_3(BF)_3(CO)_9$ are shown in Figure 2 and Tables 1 and 2. These structures include triply bridged, doubly bridged, and semibridged structures. The lowest lying triplet $Fe_3(BF)_3(CO)_9$ structure is found to lie ≥20 kcal/mol above the singlet global minimum **9−1S**. Therefore the only triplet $Fe_3(BF)_3(CO)_9$ structure considered in this paper is the lowest lying triplet **9−1T** (Figure 2).

The lowest energy $Fe_3(BF)_3(CO)_9$ structure **9−1S** (Figure 2 and Table 1) was unexpectedly found to be a triply bridged structure with nine terminal CO groups. Two μ_3-BF groups bridge all three iron atoms, and one μ-BF group bridges one edge of the Fe_3 triangle. The central Fe_3B_2 unit forms a trigonal bipyramid, and the structure has overall C_s symmetry with the symmetry plane passing through the edge-bridging μ-BF group. This $Fe_3(BF)_3(CO)_9$ structure (**9−1S**) is thus very different from the doubly edge-bridged structure of the isoelectronic $Fe_3(CO)_{12}$ (Figure 1).[13,14] The two triply bridging μ_3-BF groups in **9−1S** are predicted to exhibit relatively low ν(BF) frequencies at 1281 and 1257 cm^{-1}, whereas the single edge-bridging μ-BF group exhibits a higher ν(BF) frequency at 1364 cm^{-1} (Table 2). The equivalent Fe1−Fe1 and Fe1−Fe3 distances are 2.642 Å (B3LYP) or 2.608 Å (BP86), and the unique Fe2−Fe3 distance is 2.575 Å (B3LYP) or 2.563 Å (BP86). This is consistent with the single bond to give all Fe atoms the favored 18-electron configurations. For comparison, the experimental Fe−Fe distances determined by X-ray crystallography[14] for $Fe_3(CO)_{12}$ (= $Fe_3(CO)_{10}(\mu\text{-}CO)_2$) are 2.68 Å for the two unbridged edges and 2.56 Å for the unique doubly bridged edge.

The $Fe_3(BF)_3(CO)_9$ structure **9−1S** is obviously a very favorable $Fe_3(BF)_3(CO)_9$ structure since the next higher lying $Fe_3(BF)_3(CO)_9$ structure, namely, the C_1 structure **9−2S** (Figure 2 and Table 1), lies 19.1 kcal/mol (B3LYP) or 24.3 kcal/mol (BP86) above **9−1S**. Structure **9−2S** is related to the experimentally known doubly bridged $Fe_3(CO)_{12}$ structure (Figure 1) by replacing both bridging CO groups and one of the terminal CO groups with BF ligands, so that one of the edges of the Fe_3 triangle in **9−2S** is bridged by two μ-BF groups. However, one of these edge-bridging μ-BF groups has a weaker interaction with the third iron atom with a B−Fe1 distance of 2.517 Å (B3LYP) or 2.387 Å (BP86) as compared with the shorter B−Fe2 and B−Fe3 distances of 1.971 Å (B3LYP) or 2.010 Å (BP86) and 2.011 Å (B3LYP) or 2.021 Å (BP86), respectively. This "semi-face bridging" BF group in **9−2S** exhibits a ν(BF) frequency of 1268 cm^{-1} (Table 2), which is in the same region as the two μ_3-BF groups in **9−1S**. The second edge-bridging μ-BF group in **9−2S** has a very long Fe···B distance to the third iron atom and exhibits a ν(BF) frequency at 1342 cm^{-1}, which is in essentially the same region as that of the edge-bridging BF group in **9−1S**. The terminal BF group in **9−2S** exhibits a still higher ν(BF) frequency at 1480 cm^{-1}. In the essentially isosceles Fe_3 triangle of **9−2S**, the two equivalent nonbridged edges are 2.720 Å (B3LYP) or 2.686 Å (BP86), and the two doubly BF-bridged edges are 2.597 Å (B3LYP) or 2.575 Å (BP86). All three of these edge-lengths correspond to formal Fe−Fe single bonds with the unbridged edges being appreciably longer than the doubly bridged edge in accord with expectation. The three Fe−Fe single bonds give all three iron atoms in **9−2S** the favored 18-electron configuration.

A third doubly bridged $Fe_3(BF)_3(CO)_9$ structure **9−3S** (Figure 2 and Table 1) is even more closely related to the known $Fe_3(CO)_{12}$ structure[13,14] in that the boron atoms of neither of the edge-bridging μ-BF groups are close to

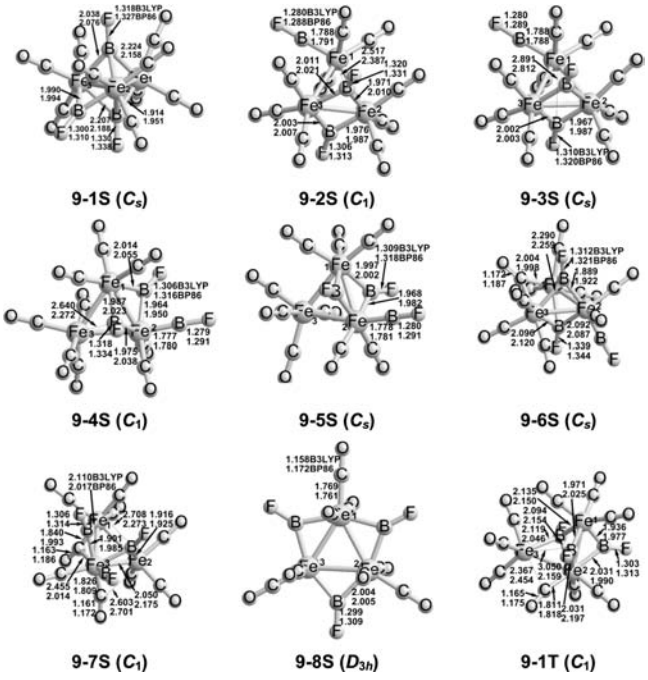

Figure 2. Nine optimized structures structures for $Fe_3(BF)_3(CO)_9$ (eight singlets and one triplet). Bond distances are reported in angstrom, with the upper numbers being B3LYP distances and the lower numbers BP86 distances.

(44) Dunning, T. H. *J. Chem. Phys.* **1970**, *53*, 2823.
(45) Dunning, T. H.; Hay, P. J. *Methods of Electronic Structure Theory*; Schaefer, H. F., Ed.; Plenum: New York, 1977; pp 1−27.
(46) Huzinaga, S. *J. Chem. Phys.* **1965**, *42*, 1293.
(47) Wachters, A. J. H. *J. Chem. Phys.* **1970**, *52*, 1033.
(48) Hood, D. M.; Pitzer, R. M.; Schaefer, H. F. *J. Chem. Phys.* **1979**, *71*, 705.
(49) Frisch, M. J. et al. *Gaussian 03*, Revision D 01; Gaussian, Inc: Wallingford, CT, 2004 (see Supporting Information for details).
(50) Papas, B. N.; Schaefer, H. F. *J. Mol. Struct.* **2006**, *768*, 275.

Table 1. Total Energies (E, in Hartree), Relative Energies (ΔE, in kcal/mol), Numbers of Imaginary Vibrational Frequencies (Nimag), and Fe−Fe Distances (in Å) for $Fe_3(BF)_3(CO)_9$

	B3LYP						BP86					
	$-E$	ΔE	Nimag	Fe−Fe distances			$-E$	ΔE	Nimag	Fe−Fe distances		
9−1S (C_s)	5185.94360	0.0	0	2.642	2.642	2.575	5186.69640	0.0	0	2.608	2.608	2.563
9−2S (C_1)	5185.91321	19.1	0	2.720	2.723	2.597	5186.65769	24.3	0	2.686	2.686	2.575
9−3S (C_s)	5185.91278	19.3	32*i*	2.725	2.731	2.594	5186.65643	25.1	38*i*	2.688	2.691	2.576
9−4S (C_1)	5185.91154	20.1	0	2.586	2.735	2.727	5186.65781	24.2	0	2.581	2.675	2.648
9−5S (C_s)	5185.91115	20.4	27*i*	2.581	2.747	2.735	5186.65383	26.7	51*i*	2.569	2.719	2.705
9−6S (C_s)	5185.90876	21.9	22*i*	2.629	2.568	2.629	5186.66112	22.1	0	2.602	2.543	2.602
9−7S (C_1)	5185.90794	22.4	0	2.803	2.661	2.625	5186.65521	25.8	0	2.681	2.531	2.656
9−8S (D_{3h})	5185.90730	22.8	0	2.699	2.699	2.699	5186.64877	29.9	0	2.675	2.675	2.675
9−1T (C_1)	5185.91215	19.7	0	2.597	3.390	2.611	5186.64906	29.7	0	2.607	2.930	2.500

Table 2. ν(CO) and ν(BF) Stretching Frequencies (cm^{-1}) and the Infrared Intensities (km/mol, in parentheses) for the Trinuclear $Fe_3(BF)_3(CO)_9$ Derivatives Predicted by the BP86 Method[a]

	ν(CO)	ν(BF)
9−1S (C_s)	2068(5),2031(1847),2025(1876),2008(1691),2001(100),1999(213),1972(153),1986(87),1982(37)	**1364(416),1281(197),1257(323)**
9−2S (C_1)	2059(81),2023(1960),2013(1274),1997(1775),1993(212),1990(58),1982(107),1977(97),1950(213)	1480(625),**1342(278),1268(289)**
9−3S (C_s)	2060(82),2024(1954),2015(1285),1997(1711),1993(199),1990(75),1983(95),1977(102),1958(275)	1479(611),**1327(49),1304(480)**
9−4S (C_1)	2063(323),2025(1832),2010(1371),2000(1359),1996(48),1989(125),1984(231),1981(108),1913(256)	1480(622),**1336(293),1256(269)**
9−5S (C_s)	2065(335),2020(1918),2006(1177),2000(1911),1995(72),1989(58),1987(32),1977(258),1968(60)	1478(615),**1337(76),1315(505)**
9−6S (C_s)	2064(126),2030(1719),2019(1872),2006(781), 2001(112),1987(402),1977(4),**1871(410)**	1466(618),**1317(275),1223(250)**
9−7S (C_1)	2061(218),2024(1701),2016(1849),2003(534),1994(520),1989(398),1979(155),1968(86),**1875(230)**	1483(705),**1344(444),1216(192)**
9−8S (D_{3h})	2063(323),2024(1167),2024(1167),2004(2518),1996(0),1983(311),1983(311),1966(0),1966(0)	**1365(0),1333(843),1333(843)**
9−1T (C_1)	2057(7),2019(1679),2010(2130),2001(1782),1992(278),1991(55),1988(163),1977(215),1952(185)	**1349(446),1281(202),1253(314),**

[a] The bridging ν(CO) and ν(BF) frequencies are reported in **bold type**.

the third iron atom. Both of these bridging BF groups are thus true edge-bridging groups exhibiting ν(BF) frequencies of 1327 and 1304 cm^{-1}, similar to the true edge-bridging μ-BF groups in the $Fe_3(BF)_3(CO)_9$ structures **9−1S** and **9−2S**. Structure **9−3S** lies 19.3 kcal/mol (B3LYP) or 25.1 kcal/mol (BP86) above the global minimum **9−1S** and has an imaginary vibrational frequency of 32*i* cm^{-1} (B3LYP) or 38*i* cm^{-1} (BP86). Following the corresponding normal mode leads from **9−3S** to **9−2S**, with the boron atom of one of the two edge-bridging μ-BF groups approaching within the semibonding distance of the third iron atom as noted above.

The pair of singlet $Fe_3(BF)_3(CO)_9$ structures **9−4S** and **9−5S** is analogous to the pair of structures **9−2S** and **9−3S**, respectively, except for the location of the terminal BF group relative to the $Fe_2(\mu\text{-BF})_2$ bridged edge (Figure 2 and Table 1). Thus, in the structure pair **9−2S**/**9−3S** the terminal BF group is bonded to the iron atom not associated with the doubly bridged Fe−Fe edge. However, in the structural pair **9−4S**/**9−5S** the terminal BF group is bonded to one of the iron atoms in the doubly bridged Fe−Fe edge. The energy difference associated with this subtle change is rather small (<2 kcal/mol). Structure **9−5S**, at 20.4 kcal/mol (B3LYP) or 26.7 kcal/mol (BP86) above **9−1S**, exhibits an imaginary vibrational frequency at 27*i* cm^{-1} (B3LYP) or 51*i* cm^{-1} (BP86). Following the corresponding normal mode leads from **9−5S** to **9−4S** with a slight reduction in the energy to 20.1 kcal/mol (B3LYP) or 24.2 kcal/mol (BP86) above **9S-1**. In structure **9−4S**, as in structure **9−2S**, the boron atom of one of the edge-bridging μ-BF groups approaches within semibonding distance of 2.640 Å (B3LYP) or 2.272 Å (BP86) to the third iron atom so that this BF group becomes an incipient face-semibridging μ_3-BF group. This effectively μ_3-BF group exhibits a relatively low ν(BF) frequency of 1256 cm^{-1} (Table 2), whereas the true edge-bridging μ-BF group with its boron atom far from the third iron atom exhibits a more normal bridging ν(BF) frequency of 1336 cm^{-1}. The terminal ν(BF) frequency in **9−4S**, at a still higher 1480 cm^{-1}, is essentially identical to that in **9−2S**.

The next $Fe_3(BF)_3(CO)_9$ structure, namely, the singlet **9−6S**, has two μ_3-BF groups bridging all three iron atoms as well as an edge-bridging carbonyl group (Figure 2 and Table 1). The third BF moiety in **9−6S** is a terminal BF group. Structure **9−6S**, at 21.9 kcal/mol (B3LYP) or 22.1 kcal/mol (BP86) above the global minimum **9−1S**, can be derived from **9−1S** by interchanging the bridging μ-BF group with one of the terminal carbonyl groups. This structural change makes an energy difference of >20 kcal/mol thereby showing how much more favorable bridging BF groups are relative to terminal BF groups and bridging CO groups. In **9−6S** the two μ_3-BF groups exhibit ν(BF) frequencies at 1317 and 1223 cm^{-1} whereas the terminal BF group exhibits a ν(BF) frequency at 1466 cm^{-1} (Table 2). The bridging carbonyl group in **9−6S** is predicted to exhibit a relatively low ν(CO) frequency of 1871 cm^{-1} (Table 2). The Fe_3 triangle in **9−6S** is an isosceles triangle with two edges of length 2.629 Å (B3LYP) or 2.602 Å (BP86) and a single edge of length 2.568 Å (B3LYP) or 2.543 Å (BP86). These edge lengths are very similar to those in the **9−1S** global minimum of $Fe_3(BF)_3(CO)_9$ and correspond to the formal single Fe−Fe bonds required to give all three iron atoms the favored 18-electron configuration.

The $Fe_3(BF)_3(CO)_9$ structure **9−7S**, at 22.4 kcal/mol (B3LYP) or 25.8 kcal/mol (BP86) above **9−1S**, has one μ_3-BF group bridging all three iron atoms, one edge-bridging μ-BF group, and one terminal BF group, which are predicted to exhibit ν(BF) frequencies at 1216, 1344, and 1483 cm^{-1} (Table 2). One of the carbonyl groups in **9−7S** is an edge-bridging μ-CO group predicted to exhibit a ν(CO) frequency at 1875 cm^{-1} in the typical edge-bridging carbonyl region.

The final singlet $Fe_3(BF)_3(CO)_9$ structure **9−8S** is a high symmetry (D_{3h}) structure. Structure **9−8S** lies at 22.8 kcal/mol (B3LYP) or 29.9 kcal/mol (BP86) above **9−1S** (Figure 2 and Table 1). In structure **9−8S**, the Fe_3 triangle is an equilateral triangle with edge-lengths of 2.699 Å (B3LYP) or 2.675 Å (BP86) leading to a highly symmetrical structure with the D_{3h} point group. Each edge of the Fe_3 triangle is bridged by a μ-BF group with predicted ν(BF) frequencies at 1365 and 1333 cm^{-1}, in a similar region as the edge-bridging ν(BF) frequencies of the other $Fe_3(BF)_3(CO)_9$ structures. Very symmetrical structures analogous to the $Fe_3(BF)_3(CO)_9$ structure **9−8S** are found as higher energy structures in DFT studies of $M_3(CO)_{12}$ derivatives (M = Fe,[43] Ru,[51] Os[52]) as well as $Fe_3(CS)_3(CO)_9$.

The triplet $Fe_3(BF)_3(CO)_9$ structures lie at higher energies than most of the singlet structures considered above, so only the lowest lying triplet structure, namely, **9−1T** (Figure 2 and Table 1), is considered here. This triplet structure lies 19.7 kcal/mol (B3LYP) or 29.7 kcal/mol (BP86) above the $Fe_3(BF)_3(CO)_9$ global minimum **9−1S**. Structure **9−1T** has two triply bridging μ_3-BF groups and one edge-bridging μ-BF group just like the global minimum **9−1S**. The triply bridging μ_3-BF groups in **9−1T** exhibit ν(BF) frequencies at 1281 and 1253 cm^{-1} (Table 2), which are very close to the 1281 and 1257 cm^{-1} ν(BF) frequencies of **9−1S** (Table 2). The edge-bridging μ-BF group in **9−1T** exhibits a ν(BF) frequency at 1349 cm^{-1}, which also is very close to the corresponding 1364 cm^{-1} ν(BF) frequency of the edge-bridging μ-BF group in **9−1S**. The major difference between **9−1T** and **9−1S** is that one of the Fe···Fe distances in **9−1T** (Table 1) of 3.390 Å (B3LYP) or 2.930 Å (BP86) is too long for an Fe−Fe bond (Fe1···Fe3 in Figure 2) so that the Fe_3 triangle in **9−1T** only has two Fe−Fe bonds rather than three Fe−Fe bonds as in all of the eight singlet $Fe_3(BF)_3(CO)_9$ structures. This lack of an Fe−Fe bond in the triplet **9−1T** gives two of the three iron atoms only a 17-electron configuration, consistent with the triplet spin multiplicity.

3.2. Molecular Orbital Analysis. To interpret the nature of the Fe−B bonds in the global minimum $Fe_3(BF)_3(CO)_9$ structure **9−1S**, the nine highest occupied molecular orbitals are displayed in Figure 3.

In the C_s structure **9−1S**, one of the three iron atoms is in the reflection plane and the two other iron atoms are out of the plane. The highest occupied molecular orbital (HOMO, a″) involves the d_{xz} orbitals from the two out-of-plane iron atoms with a symmetry suitable for the $\pi^*(x)$ orbital of one of the μ_3-BF ligands, and forms two of the three bridging Fe−B bonds. The HOMO-1 (a′) orbital involves the d_{z^2} orbital of the in-plane iron atom overlapping with two $\pi^*(y)$ orbitals from each of the two μ_3-BF ligands, and forms two bridging Fe−B bonds (i.e., the same Fe atom with two μ_3-B atoms). The HOMO-2 (a′) orbital involves the d_{z^2} orbitals from the two out-of-plane iron atoms, and forms two bridging Fe−B bonds with the $\pi^*(x)$ orbital of the μ_2-BF ligand, as well as two bridging Fe−B bonds with the $\pi^*(x)$ orbital of the other μ_3-BF ligand (other than the μ_3-BF ligand of the HOMO). An additional eighteen bonding molecular orbitals (including HOMO-3 to HOMO-8 in Figure 3 and other MOs with lower energies not displayed in Figure 3) have been examined. None of them is essentially related to any Fe−B bonding.

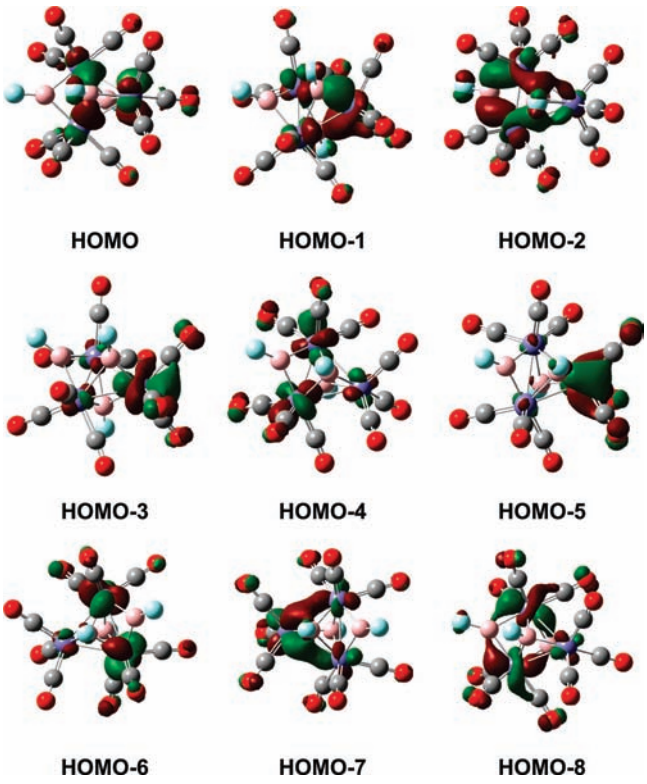

Figure 3. Nine highest occupied molecular orbitals of the $Fe_3(BF)_3(CO)_9$ structure **9−1S** at the B3LYP/DZP level.

The above MO analysis shows that the back-bonding from the atomic d orbitals of the iron atoms to the antibonding π^* orbitals of the BF ligands plays an important role in the bridging Fe−B bonds.

4. Discussion

The structure of the global minimum **9−1S** of $Fe_3(BF)_3(CO)_9$ (Figure 2) is very different from any of the structures previously found for the homoleptic trimers $M_3(CO)_{12}$ (M = Fe, Ru, Os) by any of the previous theoretical studies, even the higher energy structures. The novel feature of structure **9−1S** is the presence of two μ_3-BF groups, one on the top and the other one on the bottom of the Fe_3 triangle. The two μ_3-BF groups form an Fe_3B_2 trigonal bipyramid with the Fe_3 triangle. No structures of the homoleptic derivatives $M_3(CO)_{12}$ containing the analogous μ_3-CO groups were found in the previous theoretical studies[43,51,52] even though such μ_3-CO groups are known in other organometallic structures such as the very stable[53] $(\eta^5\text{-}C_5H_5)_3Ni_3(\mu_3\text{-}CO)_2$. However, the BCl group in the crystallographically characterized complex $[AsPh_4][Fe_3(CO)_9(\mu\text{-}CO)(\mu_3\text{-}HBCl)]$ is a triply bridging group accompanied by a bridging H atom.[54]

(51) Peng, B.; Li, Q.-S.; Xie, Y.; King, R. B.; Schaefer, H. F. *Dalton Trans.* **2008**, 6977.
(52) Li, Q.-S.; Xu, B.; Xie, Y.; King, R. B.; Schaefer, H. F. *Dalton Trans.* **2007**, 4312.
(53) Byers, L. R.; Uchtman, V. A.; Dahl, L. F. *J. Am. Chem. Soc.* **1981**, *103*, 1942.
(54) Crascall, L. E.; Thimmappa, B. H. S.; Rheingold, A. L.; Ostrander, R.; Fehlner, T. P. *Organometallics* **1994**, *13*, 2153.

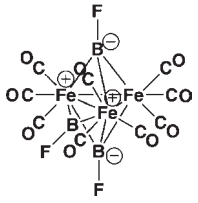

Figure 4. Formal charge distribution in the lowest energy $Fe_3(BF)_3(CO)_9$ structure **9−1S**.

The tendency for BF ligands to bridge three metal atoms as in structure **9−1S** for $Fe_3(BF)_3(CO)_9$ can be related to the reluctance to form B−F multiple bonds. With a single B−F bond, the boron atom in a μ_3-BF group bridging three metal atoms has approximate tetrahedral coordination analogous to the boron atoms in the well-known anions BX_4^- (X = H, F, C_6H_5, etc.). This leads to a formal negative charge on the boron atom of a μ_3-BF group, as shown schematically in Figure 4 for the lowest energy $Fe_3(BF)_3(CO)_9$ structure **9−1S**. The two formal negative charges on the boron atoms of the μ_3-BF groups are balanced by formal positive charges on two of the iron atoms in the Fe_3 triangle. Such a μ_3-BF group is thus very effective in removing negative charge from the triangle of low formal oxidation state iron atoms. A similar situation does not occur for a carbonyl group because of the much greater tendency to form C=O double bonds relative to forming B=F double bonds. Such B=F double bonds require the unfavorable feature of a formal positive charge on the highly electronegative fluorine atom.

The four next higher energy singlet $Fe_3(BF)_3(CO)_9$ structures, namely, **9−2S**, **9−3S**, **9−4S**, and **9−5S** (Figure 2), are all related to the lowest energy $Fe_3(CO)_{12}$ structure with two edge-bridging carbonyl groups by replacing both bridging carbonyl groups with edge-bridging μ-BF groups as well as one of the terminal carbonyl groups with a terminal BF group (Figure 1). The exact analogues are structures **9−3S** and **9−5S**, which differ only in the location of the terminal BF group relative to the doubly BF-bridged Fe−Fe edge. However, these structures are not true minima since they have small imaginary vibrational frequencies of 20*i* to 50*i* cm^{-1} by either method. Following the corresponding normal modes leads **9−3S** to **9−2S** and **9−5S** to **9−4S**. In both cases the boron atom of one of the edge-bridging μ-BF groups moves toward the iron in the Fe_3 triangle not part of the doubly bridged Fe−Fe edge (Figure 5). This generates an unsymmetrical μ_3-BF group with the newly formed Fe--B distance of 2.517 Å (B3LYP) or 2.387 Å (BP86) for **9−2S** and 2.640 Å (B3LYP) or 2.272 Å (BP86) for **9−4S**, significantly longer than the other Fe−B distances of 2.00 ± 0.03 Å.

The lowest energy structures for $M_3(CO)_{12}$ (M = Ru, Os) have all terminal carbonyl groups (Figure 1).[15−17] No

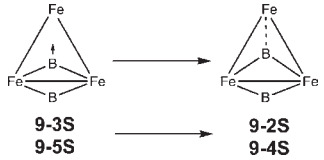

Figure 5. Conversion of one of the edge-bridging μ-BF groups in **9−3S** or **9−5S** into a face-semibridging μ_3-BF group in **9−2S** or **9−4S**, respectively.

corresponding $Fe_3(BF)_3(CO)_9$ structures were found in which all three BF groups and all nine carbonyl groups are terminal carbonyl groups. This again shows the reluctance of the fluoroborylene (BF) group to function as a terminal ligand.

In summary, the singular example of $Fe_3(BF)_3(CO)_9$ provides an excellent illustration of the difference between the isoelectronic fluoroborylene (BF) and carbonyl (CO) groups in their bonding to transition metals. In this connection the following observations are significant:

(1) Two face-bridging μ_3-BF groups are found in the lowest energy structure of $Fe_3(BF)_3(CO)_9$ (**9-1S** in Figure 2) whereas analogous face-bridging μ_3-CO groups have never been found in any of the $M_3(CO)_{12}$ structures (M = Fe, Ru, Os);

(2) Structures $Fe_3(BF)(CO)_9(\mu\text{-BF})_2$ with two BF groups bridging one of the edges of the Fe_3 triangle analogous to the lowest energy $Fe_3(CO)_{10}(\mu\text{-CO})_2$ structure for $Fe_3(CO)_{12}$ are not true minima but transition states with a single imaginary vibrational frequency in the range 20*i* to 50*i* cm^{-1}. Following the corresponding normal mode converts one of the edge-bridging μ-BF groups to an essentially face-bridging μ_3-BF group.

(3) No $Fe_3(BF)_3(CO)_9$ structures with exclusively terminal BF and CO groups are found at accessible energies in contrast to the lowest energy structures of $M_3(CO)_{12}$ (M = Ru, Os) with exclusively terminal carbonyl groups.

Acknowledgment. We are indebted to the 111 Project (B07012) in China, the National Natural Science Foundation of China (Grant 20973066), and the U.S. National Science Foundation (Grants CHE-0749868 and CHE-0716718) for support of this research.

Supporting Information Available: Tables S1−S5: Theoretical harmonic vibrational frequencies for $Fe_3(BF)_3(CO)_9$ (9 structures) from B3LYP/DZP and BP86/DZP method. Tables S6−S14: Theoretical Cartesian coordinates for $Fe_3(BF)_3(CO)_9$ (9 structures), using the B3LYP/DZP method and BP86/DZP method. Complete Gaussian 03 reference (reference 49). This material is available free of charge via the Internet at http://pubs.acs.org.